Nucleic Acids Research, 2006, Vol. 34, No. 8 ***2445–2454***
doi:10.1093/nar/gkl276

Characterization of long RNA-cleaving deoxyribozymes with short catalytic cores: the effect of excess sequence elements on the outcome of *in vitro* selection

Kenny Schlosser, Jeffrey C.F. Lam and Yingfu Li*

Department of Biochemistry and Biomedical Sciences and Department of Chemistry, McMaster University, Hamilton, Canada L8N 3Z5

Received March 6, 2006; Revised March 27, 2006; Accepted April 4, 2006

ABSTRACT

We previously conducted an *in vitro* selection experiment for RNA-cleaving deoxyribozymes, using a combinatorial DNA library containing 80 random nucleotides. Ultimately, 110 different sequence classes were isolated, but the vast majority contained a short 14–15 nt catalytic DNA motif commonly known as 8–17. Herein, we report extensive truncation experiments conducted on multiple sequence classes to confirm the suspected catalytic role played by 8–17 and to determine the effect of excess sequence elements on the activity of this motif and the outcome of selection. Although we observed beneficial, detrimental and neutral consequences for activity, the magnitude of the effect rarely exceeded 2-fold. These deoxyribozymes appear to have survived increasing selection pressure despite the presence of additional sequence elements, rather than because of them. A new deoxyribozyme with comparable activity, called G15–30, was ~2.5-fold larger and experienced a ~4-fold greater inhibitory effect from excess sequence elements than the average 8–17 motif. Our results suggest that 8–17 may be less susceptible to the potential inhibitory effects of excess arbitrary sequence than larger motifs, which represents a previously unappreciated selective advantage that may contribute to its widespread recurrence.

INTRODUCTION

In vitro selection or SELEX (1–3), is based on the fundamental assumption that functional DNA or RNA molecules can be found in a pool of random nucleic acid sequences. This assumption has been experimentally validated on numerous occasions since 1990, with the isolation of hundreds of deoxyribozyme, ribozyme and aptamer sequences. However, there are still unanswered questions regarding the distribution of functional nucleic acids in sequence space, and more importantly, how best to access them.

Every new *in vitro* selection experiment begins with a combinatorial library of single-stranded DNA molecules. The prevailing view supported by several theoretical studies is that longer libraries offer greater access to larger modular motifs with greater structural complexity (4–6), which in turn may be correlated with greater functional activity (7). However, the tangible benefits of longer random libraries are somewhat ambiguous given the fact that both long and short libraries (from >200 nt to <30 nt; nt: nucleotide) have yielded functional molecules. Assessing the true merits of longer random libraries is made even more difficult by the presence of excess sequence elements that often mask a shorter functional motif, often with equal or greater activity than the full-length precursor. Examples of this scenario are abundant in the literature, suggesting that this is both a significant and general phenomenon that applies to different types of reactions for both functional DNA (8–13) and RNA (14–26).

The presence of excess sequence elements has been especially relevant to the selection of one very well known RNA-cleaving deoxyribozyme, called 8–17. The 8–17 motif measures just 14–15 nt in length, but has been repeatedly isolated in several independent selection experiments using random libraries greater than or equal to 40 nt (27–32). Previously, we conducted an *in vitro* selection experiment using a DNA library that featured the longest random-sequence domain (80 nt) ever used for the isolation of RNA-cleaving deoxyribozymes (33). Our primary motivation for choosing this length was to increase the probability of isolating a diverse collection of deoxyribozymes. For the same reason, we used several reaction times during the course of selection (from as long

*To whom correspondence should be addressed. Tel: 1 905 5259140; Fax: 1 905 522 9033; Email: liying@mcmaster.ca

as 5 h to as short as 5 s) to promote phenotypic heterogeneity across different generations, and sequenced many clones from these different generations in an effort to thoroughly assess the population diversity. Ultimately, 110 different sequence classes were identified, but >90% of these contained variants of the 8–17 motif, which we suspected might be responsible for the observed catalytic activity. Peracchi (31) has previously demonstrated that catalysis in the Mg5 RNA-cleaving deoxyribozyme is likely supported by an 8–17 motif, contrary to the much larger secondary structure originally proposed by Famulok and colleagues (29).

While the mere presence of the 8–17 motif is highly suggestive given its recurrence in other studies, we wondered if it might represent just one module within a larger, more sophisticated structure. For instance, Silverman and colleagues (13) re-isolated the catalytic core of a short RNA ligase deoxyribozyme whose activity benefited by more than an order of magnitude from the presence of ~20 additional nucleotides. Our objective in this study was 3-fold. We wanted to (i) substantiate the suspected catalytic role played by the 8–17 motifs, (ii) determine how their activity was affected by excess sequence elements and (iii) determine what kind of impact this had on the outcome of selection. This knowledge could have general implications for the effective design and implementation of future *in vitro* selection efforts.

MATERIALS AND METHODS

Oligonucleotides and reagents

Oligonucleotides were prepared by automated DNA synthesis using cyanoethylphosphoramidite chemistry (Keck Biotechnology Resource Laboratory, Yale University; Mobix Central Facility, McMaster University). DNA and RNA oligonucleotides were purified by 10% preparative denaturing (8 M urea) PAGE and their concentrations were determined by spectroscopic methods.

Nucleoside 5′-triphosphates and [γ-^{32}P]ATP were purchased from Amersham Pharmacia. T4 DNA ligase, T4 polynucleotide kinase (PNK), calf intestine alkaline phosphatase and T7 RNA polymerase were purchased from MBI Fermentas. All chemical reagents were purchased from Sigma. The 50 nt RNA substrate (S) was produced by *in vitro* transcription using T7 RNA polymerase and an appropriate double-stranded DNA template generated by PCR as described previously (33), and standard *in vitro* transcription protocols were used with pairs of complementary synthetic DNA oligos to produce the 26 nt SS substrate, and 18 nt ST substrate. Nucleotide sequences of RNA substrates are as follows: 50 nt S = 5′-ggagagagaugggugcguuacguaaaacuuacaucuacgaaucagguucga; 26 nt SS = 5′-ggagagagaugggugcguuacguaaa; 18 nt ST substrate = 5′-gggagagaugggugcguu.

Construction of substrate-deoxyribozyme cis constructs

The 50 nt or 26 nt RNA substrates were first ligated to 14 nt A1 (5′-ggaaactagacaga) in a separate large-scale ligation reaction. Typically, 2500 pmol of RNA substrate was combined with 2750 pmol ligation template (5′-tctctctcctctgtctag) and 3000 pmol of A1, heated for 30 s at 90°C and allowed to cool at room temperature for ~10 min. After cooling, 10 µl of 10× ligase buffer (supplied by Fermentas) and 10 µl of T4 DNA ligase (5 Weiss U/µl) were added to initiate the ligation reaction. The reaction mixture (100 µl, total volume) was incubated at room temperature for 4 h or overnight. The ligated A1-RNA substrate was recovered by standard ethanol precipitation and purified by 10% denaturing PAGE. The A1-RNA substrate construct was 5′-^{32}P-labelled with PNK, extracted twice with phenol/chloroform/isoamyl alcohol (25:24:1), and ethanol precipitated before being used in separate small-scale ligation reactions with specific deoxyribozymes. Thirty pmol of A1-substrate was combined with 90 pmol of 5′-phosphorylated deoxyribozyme, 36 pmol of ligation template (5′-gcgtacgtgtcgaacctgattcg), and 45 pmol of substrate cleavage blocker (5′-tttacgtaacgcacccatctctctcctctgtctag), heated at 90°C for 30 s and allowed to cool at room temperature for ~5–10 min. The substrate cleavage blocker is synthetic DNA complementary to a section of the RNA substrate surrounding the cleavage site, and was used to prevent deoxyribozyme-mediated cleavage during ligation. After cooling, 1.25 µl of 10× ligase buffer (supplied by Fermentas), 4 µl of T4 DNA ligase (5 Weiss U/µl) and DEPC treated H_2O were added to a final volume of 25 µl. The reaction was incubated at 37°C for 1 h, then ethanol precipitated and purified by 10% denaturing PAGE.

Kinetic analyses of cis-cleaving deoxyribozymes

A typical intramolecular self-cleavage assay consisted of the following steps: (i) heat denaturation of the deoxyribozyme-substrate construct in water for 30 s at 90°C, followed by slow cooling at room temperature for ~10 min, (ii) the addition of selection buffer (final concentration, 400 mM NaCl, 100 mM KCl, 7.5 mM $MgCl_2$, 7.5 mM $MnCl_2$, 50 mM HEPES, pH 7.0 at 23°C) and incubation at room temperature for a designated period of time, (iii) addition of EDTA to 30 mM to stop the reaction, (iv) separation of cleavage products by denaturing 10% PAGE and (v) quantitation using a PhosphorImager and ImageQuant software. Time courses for each deoxyribozyme were conducted at least twice using 13–16 different time points for each. The experimental data was fit to either a single, $Y = Y_{max}(1 - e^{(-k_{obs}t)})$, or double, $Y = Y_{max1}(1 - e^{(-k_{obs1}t)}) + Y_{max2}(1 - e^{(-k_{obs2}t)})$, exponential equation using non-linear regression analysis in GraphPad Prism 4, from which the observed rate constant (k_{obs}) and maximum cleavage yield (Y_{max}) were determined.

Kinetic analyses of trans-cleaving deoxyribozymes

For single turnover experiments, a 100-fold excess of deoxyribozyme was mixed with 5′-^{32}P-labelled substrate. Substrate and deoxyribozyme were heated together at 90°C for 30 s, and allowed to cool at room temperature for ~10 min. A 2× selection buffer was added to initiate the reaction giving a final concentration of 1.66 µM deoxyribozyme to 0.0166 µM substrate. The reaction was terminated after a designated period of time by the addition of EDTA to 30 mM. The rate constant was determined from at least two independent experiments that differed by <10%. Each time course consisted of 16 time points. A graph of fraction cleaved versus time was plotted, and the experimental data fit to a single or double exponential equation using non-linear regression analysis in GraphPad Prism 4.

RESULTS

Selection, identification and confirmation of the 8–17 catalytic motif

We previously conducted an *in vitro* selection experiment to isolate RNA-cleaving deoxyribozymes (33), using the library design illustrated in Figure 1A. In addition to 80 random deoxyribonucleotides, this library featured an RNA substrate composed of 50 fixed-sequence ribonucleotides. After performing sixteen rounds of selection, ~50 clones were sequenced from each of generations 7, 8, 10, 13 and 15, which were subjected to increasing selection pressure in the form of decreasing reaction times of 5 h, 30 min, 5 min, 30 s and 5 s, respectively. From a total sample set of 245 sequenced clones, 110 unique sequence classes were identified. On average, different classes shared only ~30% nucleotide identity, but clones within the same class boasted >90% identity. Further analysis revealed the presence of the 8–17 motif in ~94% of all classes. For simplicity, we use the term 8–17 to describe both the canonical motif (32) and all related sequence variants.

The discovery of a motif as simple and well defined as 8–17, in so many different sequences, provided a unique opportunity to gain further insight into the role of excess sequence elements during *in vitro* selection. Toward this end, 11 sequence classes were characterized in greater detail. All eight classes identified in the terminal G15 population were investigated, including one that does not contain 8–17 or any other previously characterized motif. These deoxyribozymes presumably represent the best catalysts, because they survived under the most stringent selection time. For comparison, we also selected three classes that were observed only transiently in the preceding generations 8, 10 or 13. Figure 1B shows the sequence of a specific clone from each of the ten 8–17 containing classes that were examined, as well as the frequency and generation from which they were isolated (the non-8–17 class is addressed separately in a subsequent section). The 8–17 motif has been studied extensively (27,30–32,34,35), and is readily identifiable near the 5′ end by its characteristic sequence requirements.

The secondary structure and sequence requirements of the 8–17 motif are summarized in Figure 2A. The nucleotide numbering system used in Figure 2A is analogous to the system originally proposed for the hammerhead ribozyme (36), and subsequently adopted for the 8–17 deoxyribozyme (31,34). The canonical 8–17 motif as first described by Santoro and Joyce (32), was composed of 14–15 nt (plus 7–8 nt binding arms on either side) and characterized by a G-T wobble base pair at the cleavage site, a 3 bp stem of which at least two were G-C base pairs, an invariant A_6G_7C triloop, and a single-stranded region of sequence $WC_{13}G_{14}R$ (W = A or T; R = A or G or AA). Subsequent studies have suggested that the sequence requirements of 8–17 are far more versatile. A study by Cruz *et al*. (30) reported that only four residues are strictly conserved (A_6 and G_7 in the triloop, C_{13} and G_{14} in the single-stranded turn region), the triloop region can also accept a tetraloop, the 3 bp stem can accommodate up to 1 or 2 mismatches and/or single-nucleotide bulges, and the single-stranded region has a more relaxed sequence requirement for positions W and R. Most recently, Peracchi *et al*. (34) have conducted a comprehensive mutational analysis to show the effect of different mutations on the catalytic activity of 8–17. From the results of Peracchi's study, the approximate relative activity at different nucleotide positions (in Mn^{2+} buffer) is predicted to be as follows: $T_{2.1}$>A>>G,C; C_8>T>>G,A; T_{12}>G>A>>C; $A_{15}A_{15.0}$>A>T>C>G. The magnitude and relative order of activities vary depending on the type and concentration of metal ion cofactors used. Furthermore, the composition of the 3 bp stem is also associated with varying levels of activity. The magnitudes of these effects are

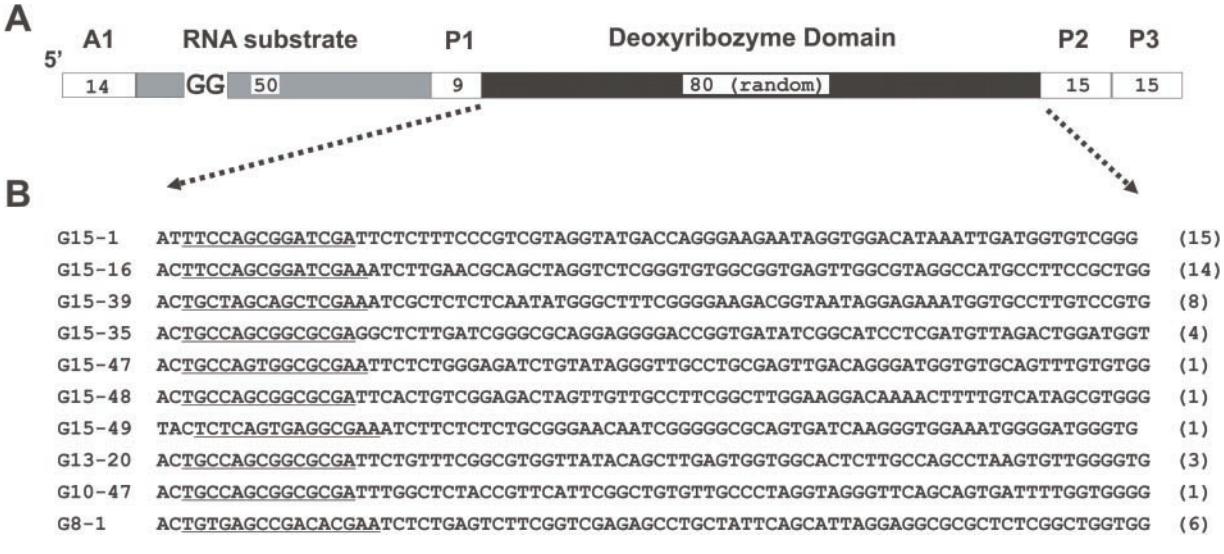

Figure 1. (**A**) Library design. Numbers indicate the nucleotide length of each section. A1 is a piece of DNA used to facilitate the separation of cleaved and non-cleaved molecules in our gel-based selection method. The total length of the RNA substrate is 50 nt (see Materials and Methods for nucleotide sequence), and cleavage occurs at the 5′ $G_{11}G_{12}$ junction. P1, P2 and P3 represent primer binding sites. P1 was used from G0-G16, P2 was used from G0-G7, and P3 was used from G8-G16. The putative deoxyribozyme domain contains 80 random nucleotides. (**B**) Sequences of specific clones from selected deoxyribozymes classes. Only the random sequence domain is shown. Each sequence is preceded by a numeric designation that indicates the generation from which it was taken (i.e. G#), and the specific clone number. Bracketed numbers at the far right of each sequence indicate the number of clones observed in that generation.

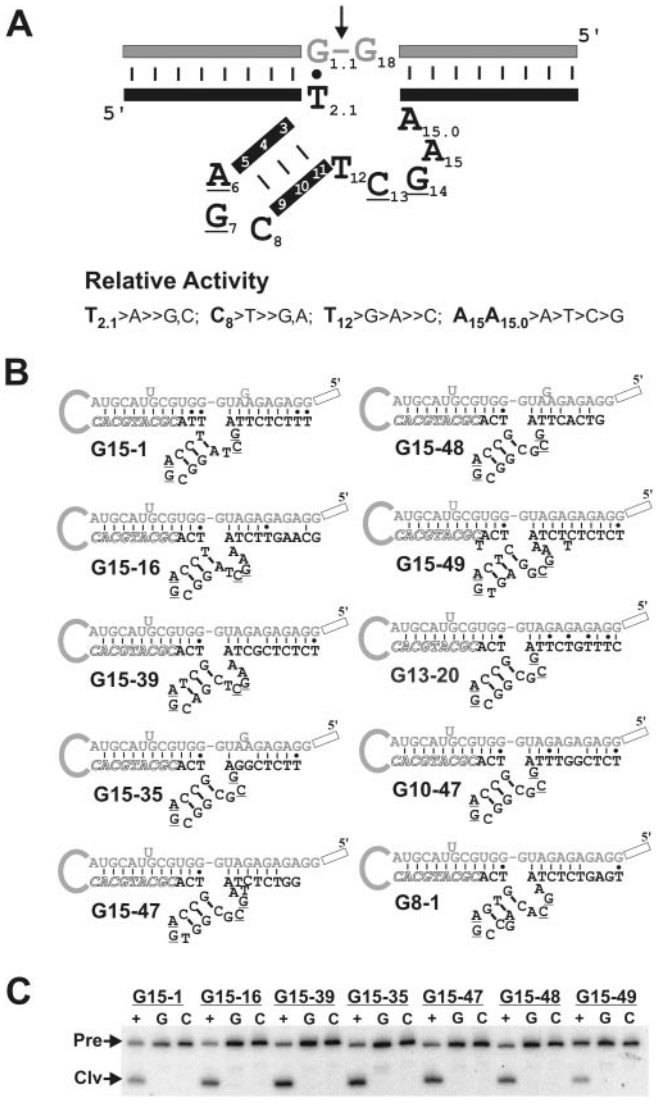

Figure 2. (**A**) Graphical summary of the 8–17 secondary structure and sequence requirements. The 8–17 motif is characterized by a G-T wobble base pair (black dot) at the cleavage site, a 3 base pair stem, a tri-loop and a 4–5 nt single-stranded turn region. Two general binding arms on either side of the 8–17 motif (thick black lines) engage the substrate strand (thick grey lines) through Watson–Crick base pairs (indicated by thin black lines). Underlined nucleotides are strictly conserved, while mutations at other positions are acceptable but associated with different catalytic activity. The approximate relative activity (in Mn^{2+} buffer) at different positions is indicated. The magnitude and relative order of activities may vary depending on the type of metal ion cofactors used. Cleavage occurs at the G-G junction indicated by the arrow, although it has been previously shown that 8–17 variants can collectively cleave 14 of 16 possible dinucleotide junctions. (**B**) Proposed secondary structure interaction between the deoxyribozyme domain (black letters) and the RNA substrate domain (grey line/letters) of each sequence class. The outlined letters correspond to P1 and the outlined box corresponds to A1. For simplicity, only the 8–17 containing section of the deoxyribozyme domain is shown. (**C**) Evidence to support a catalytic role by 8–17. The autoradiogram depicts the results of self-cleavage assays for truncated versions of each sequence class. The positive control (+) refers to the truncated sequence shown in (B) with a truncated RNA substrate lacking 24 nt from the 3′ end (30 min reaction time). Mutants having either a G_7 to T or C_{13} to T mutation are denoted by G and C, respectively (12 h reaction time). Cleavage products (Clv) were separated from the uncleaved precursor substrate (Pre) by 10% denaturing PAGE.

omitted since the assay conditions in reference (34) are not directly comparable to our own.

The suspected secondary structure interaction between the 8–17 containing DNA domain and the RNA substrate are illustrated in Figure 2B for each class. Approximately 91% of all the observed 8–17 motifs were located at the 5′ end of the DNA domain, which allowed them to exploit the 5′ primer-binding site (P1) as one binding arm. This unintentional sequence complementarity likely favoured the selection of catalysts that cleave the adjacent G-G dinucleotide junction. Although the observed 8–17 motifs satisfy the sequence requirements established by previous studies, formation of the 8–17 motif is not predicted to be the most energetically favourable according to secondary structure prediction software, such as mfold (37). This discrepancy is maintained even when full-length molecules are truncated to remove excess sequence elements. Therefore, we synthesized 3′ truncated enzymes corresponding to the nucleotide sequences shown in Figure 2B (containing only the suspected 8–17 motif and 8–10 nt binding arms), and ligated them to a truncated RNA substrate lacking 24 consecutive nucleotides from the 3′ end (corresponding to the loop region that is not expected to interact with the deoxyribozyme domain). Figure 2C indicates that these truncation derivatives are still catalytically active, but the same constructs containing either a G_7 to T substitution, or a C_{13} to T substitution are completely inactive. These experimental results are consistent with theoretical expectations (both G_7 and C_{13} are known to be invariant nucleotides), and strongly support a catalytic role for the embedded 8–17 motif.

To assess the effect of excess sequence elements on the activity of the 8–17 motif, four different constructs were made for each sequence class, which are depicted in Figure 3. These constructs include: (i) the full-length enzyme, denoted by 'L', (ii) a 3′ truncated enzyme containing only the 8–17 motif and an 8–10 nt 3′ substrate binding arm (corresponding to the sequences shown in Figure 2B), denoted by 'S' (iii) the same truncated enzyme from part ii with a truncated

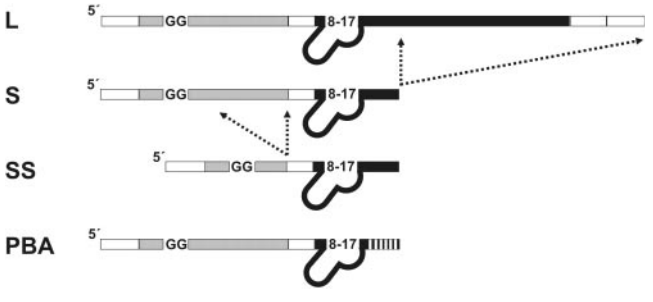

Figure 3. Schematic diagram of different truncation constructs that were assayed. Dotted arrows define truncation regions. L corresponds to the original full-length molecule. S corresponds to a 3′ truncated construct containing only the 8–17 motif and an 8–10 nt 3′ binding arm. SS corresponds to the same construct as S, but attached to a truncated RNA substrate lacking 24 contiguous nucleotides from the 3′ end. PBA corresponds to the same construct as S, but with an optimized 3′ substrate binding arm in which mismatches and bulges were replaced with Watson–Crick base pairs.

Table 1. k_{obs} and k_{rel} values of different truncation derivatives for each sequence class

Deoxyribozyme	k_{obs} (min^{-1})					k_{rel}		
	L	S	SS	PBA	PBAA	S/L	SS/S	PBAA/S
G15-1	1.0	0.83	0.76	0.10	0.65	0.8	0.9	0.8
G15-16	2.1	1.5	2.7	3.3	—	0.7	1.8	2.2
G15-39	1.7	2.1	1.8	2.0	—	1.3	0.8	0.9
G15-35*	0.87	0.90	1.2	0.06	0.72	1.0	1.3	0.8
G15-47	0.76	0.38	0.46	0.69	—	0.5	1.2	1.8
G15-48*	0.61/0.024	0.73	0.90	0.06	0.72	1.2	1.2	1.0
G15-49	0.56	0.57	0.92	1.2	—	1.0	1.6	2.1
G13-20*	0.36/0.025	0.31	0.86	0.06	0.72	0.9	2.8	2.3
G10-47*	0.24	0.36	0.45	0.06	0.72	1.5	1.2	2.0
G8-1	0.14	0.20	0.20	0.24	—	1.4	1.0	1.2
Average						1.0	1.4	1.5
Median						1.0	1.2	1.5
Maximum						1.5	2.8	2.3
Minimum						0.5	0.8	0.8

Data are the average of at least two independent trials, which typically differed by <20%. k_{rel} is defined as the activity of one construct (numerator) relative to another construct (denominator), as indicated in the table. All values have been rounded for clarity, with k_{rel} values calculated prior to rounding. G15-48 and G13-20 displayed biphasic kinetics and therefore have two different k_{obs} values representing the first and second phase, respectively. Deoxyribozymes denoted with an asterisk contain the same 8–17 catalytic core. PBAA represents the same construct as PBA, but with an extra adenosine residue in the $A_{15.0}$ position of the single-stranded turn region. Values in the PBAA/S column were determined from either the PBAA or PBA column. Reaction conditions: 400 mM NaCl, 100 mM KCl, 7.5 mM $MnCl_2$, 7.5 mM $MgCl_2$, 50 mM HEPES (pH 7.0, at 23°C) at room temperature.

Table 2. Y_{max} and $Y_{max,rel}$ values of different truncation derivatives for each sequence class

Deoxyribozyme	Y_{max} (%)					$Y_{max,rel}$		
	L	S	SS	PBA	PBAA	S/L	SS/S	PBAA/S
G15-1	72	66	45	49	66	0.9	0.7	1.0
G15-16	78	75	60	83	—	1.0	0.8	1.1
G15-39	74	76	62	85	—	1.0	0.8	1.1
G15-35*	70	66	61	42	63	0.9	0.9	1.0
G15-47	55	62	58	83	—	1.1	0.9	1.3
G15-48*	26/34	58	59	42	63	1.0	1.0	1.1
G15-49	65	21	20	76	—	0.3	1.0	3.7
G13-20*	35/32	67	76	42	63	1.0	1.1	0.9
G10-47*	66	66	69	42	63	1.0	1.0	1.0
G8-1	59	58	57	55	—	1.0	1.0	0.9
Average						0.9	0.9	1.3
Median						1.0	1.0	1.0
Maximun						1.1	1.1	3.7
Minimum						0.3	0.7	0.9

Data are the average of at least two independent trials, which typically differed by less than 5%. Y_{max} is defined as the maximum cleavage yield as determined from the best-fit curve using GraphPad Prism 4. $Y_{max,rel}$ is defined as the maximum cleavage of one construct (numerator) relative to another construct (denominator), as indicated in the table. All values have been rounded for clarity, with $Y_{max,rel}$ values calculated prior to rounding. G15-48 and G13-20 displayed biphasic kinetics and therefore have two different Y_{max} values representing the amplitude of the first and second phase, respectively. Deoxyribozymes denoted with an asterisk contain the same 8-17 catalytic core.

RNA substrate lacking 24 nt from the 3′ end, denoted by 'SS' and (iv) a 3′ truncated enzyme containing only the 8–17 motif and a perfect 3′ binding arm containing 10 consecutive Watson–Crick base pairs, denoted by 'PBA'. All rates were obtained using single-turnover cis constructs. However, each class is also active in a bimolecular trans format (Supplementary Figure 1). Table 1 summarizes the results of these truncation experiments in terms of their effect on the catalytic rate constant, k_{obs}. Since a deoxyribozyme's ability to fold into an active conformation is critical for function, we have also summarized the results of the truncation experiments in terms of their effect on the maximum cleavage yield, denoted by Y_{max} in Table 2.

Genotype to phenotype relationship

The results shown in Table 1 indicate that the catalytic rate of each class closely parallels its abundance in the population. For instance, classes such as G15-1, G15-16 and G15-39 that boast the fastest rates also represent the largest fraction of the G15 population (see Figure 1B for class frequency). In contrast, the classes that died out in earlier generations (i.e. G13-20, G10-47 and G8-1), not surprisingly, have the lowest rates. Similarly, the most abundant classes may benefit from a slight folding advantage over others, as reflected by the higher Y_{max} values shown in Table 2. The relative activity of the different 8–17 motifs is also consistent with previous reports (34).

The effect of excess sequence elements

The average effect of the excess 3′ sequence in the deoxyribozyme domain is neutral, although an even distribution of both beneficial and detrimental effects is observed (Table 1, column S/L). The magnitude of these effects, however, is relatively modest with a 50% increase or decrease in activity representing the maximum change. This modest change in activity suggests that the excess 3′ sequence is acting only to mediate the stability of 8–17's active fold, likely through the formation of the 3′ substrate-binding arm. The average effect of deleting excess sequence from the RNA substrate domain is a 40% increase in activity (Table 1, column SS/S). The activity of seven classes were inhibited by the excess ribonucleotides in varying amounts, one was neutral (G8-1), and the remainder were associated with a slightly beneficial effect (G15-1, G15-39). This variation between classes is noteworthy, since the RNA sequence is constant and presumably can form the same 5′ substrate-binding arm with P1 in each class. Therefore, the magnitude of the effect is likely influenced by downstream elements including the stability of the 3′ substrate-binding arm and perhaps even the type of 8–17 motif. On average, the activity of the G15 classes appear to be less affected by the presence of excess sequence elements in both the deoxyribozyme and substrate domains, than classes that died out in earlier generations ($k_{rel,S/L,G15avg} = 0.9$ vs. $k_{rel,S/L,<G15avg} = 1.3$; $k_{rel,SS/S,G15avg} = 1.3$ vs. $k_{rel,SS/S,<G15avg} = 1.7$). This effect closely parallels the greater stability associated with the 3′ substrate binding arm of G15 classes ($k_{rel,PBA/S,G15avg} = 1.4$ versus $k_{rel,PBA/S,<G15avg} = 1.8$).

As expected, optimized 3′ binding arms resulted in an average increase in catalytic activity (~50%), although three classes (G15-1, G15-39 and G15-35) actually decreased in activity (~10–20%), contrary to expectations (Table 1, column PBAA/S). This decrease can probably be attributed in part to experimental error, but also to the peculiarities associated with G15-1 and G15-35 (and related classes G15-48, G13-20 and G10-47). These classes have only a single adenosine residue in the terminal A_{15} position of the

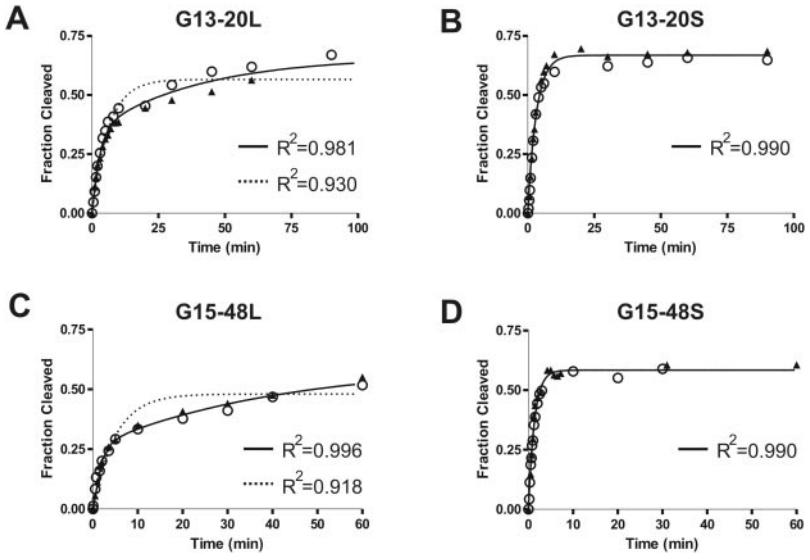

Figure 4. Kinetic analysis of G13-20 and G15-48. The fraction of substrate cleaved was plotted versus time, and the experimental data fit to either single or double exponential equations using non-linear regression analysis in GraphPad Prism 4. Two independent trials were conducted (trial 1, white circles; trial 2, black triangles), and the correlation coefficient (R^2) for the average of both trials is indicated. (**A**) G13-20L. The data are best described by a curve fit to a double exponential equation (solid black line) rather than a single exponential equation (dotted black line). (**B**) G13-20S. The data are best described by a curve fit to a single exponential equation. (**C**) G15-48L. The data are best described by a curve fit to a double exponential equation (solid black line) rather than a single exponential equation (dotted black line). (**D**) G15-48S. The data are best described by a curve fit to a single exponential equation.

single-stranded bulge region, which may base pair with the uridine residue immediately 5′ to the GG cleavage site. The extra stability conferred by the additional downstream base pairs in the perfect binding arm (PBA construct), may promote the A-U base pair to form and thereby constrain the 8–17 motif into a sub-optimal fold. Consistent with this theory, the original weaker binding arm (S construct) is associated with higher activity in these classes. Moreover, the insertion of another A residue adjacent to the existing one in the perfect binding arm (PBAA column in Tables 1 and 2) nearly restores activity to wild-type level.

Interestingly, the excess sequence elements in both the DNA and RNA domains do not seem to have a significant impact on the maximum cleavage yield. The general effect appears to be neutral, and the minor changes that are observed are likely due to inherent experimental variation. However, one class (G15-49) experiences a 70% decrease in Y_{max} after deletion of its excess 3′ DNA sequence, the magnitude of which cannot be explained by simple experimental variation. Instead, we suspect the disruptive effect of the two T bulges in the 5′ and 3′ binding arms is attenuated by the presence of the downstream DNA sequence, and intensified in its absence. The downstream sequence elements may form additional stabilizing contacts with A1. Consistent with this theory, Y_{max} is ~3.7-fold larger when both T bulges are removed in G15-49 PBA.

Characterization of the global 8–17 population

We wondered if the results of our 10 deoxyribozyme sample set were representative of the global 8–17 population from our selection experiment. On average, a neutral or modest inhibitory effect was observed with excess sequence elements in the deoxyribozyme and substrate domains, respectively. However, we might expect that the G15 classes would have been selected, in part, for their ability to minimize any negative effect associated with excess sequence elements. To address this issue, we looked for the six different 8–17 variants from G15 (G15-35 and G15-48 have the same 8–17 core motif) in the other ~100 sequence classes that were eliminated during earlier generations under more permissive selection conditions. Most of these fast 8–17 variants were unique, and not observed in other generations. However, the 8–17 catalytic core from G15-1 was also present in G13-E78, and G15-35 shares the same core motif with G15-48, G13-20, G10-47 and G7-E33. We determined that the full-length G13-E78 deoxyribozyme has a k_{obs} of 1.09 min^{-1}, and a Y_{max} of 66%. Therefore, G13-E78 was not eliminated because of an uncharacteristically large inhibitory effect from excess sequence elements. We suspect G13-E78's absence from the generation 15 population may be due to sampling error, PCR bias, sub-sampling effects or some combination thereof.

Classes G15-35 and G15-48 are 2–3 times faster than G13-20 and G10-47 even though they contain the same 8–17 catalytic core. The disparity between their rates, however, can be explained by the difference in their 3′ substrate binding arms. Both G13-20 and G10-47 have relatively poor 3′ substrate binding arms as reflected by the ~2-fold higher activity observed upon optimization (Table 1, PBAA/S column). This contrasts with G15-35 and G15-48, which experience an approximately neutral effect upon optimization of their 3′ substrate binding arms. It should be noted that G15-48 and G13-20 appear to follow biphasic kinetics, which are characterized by a fast initial phase followed by a slower second phase. Though not particularly common, biphasic kinetics have been observed previously in other deoxyribozymes (38), and ribozymes like the hairpin (39,40) in which it was attributed to the formation of

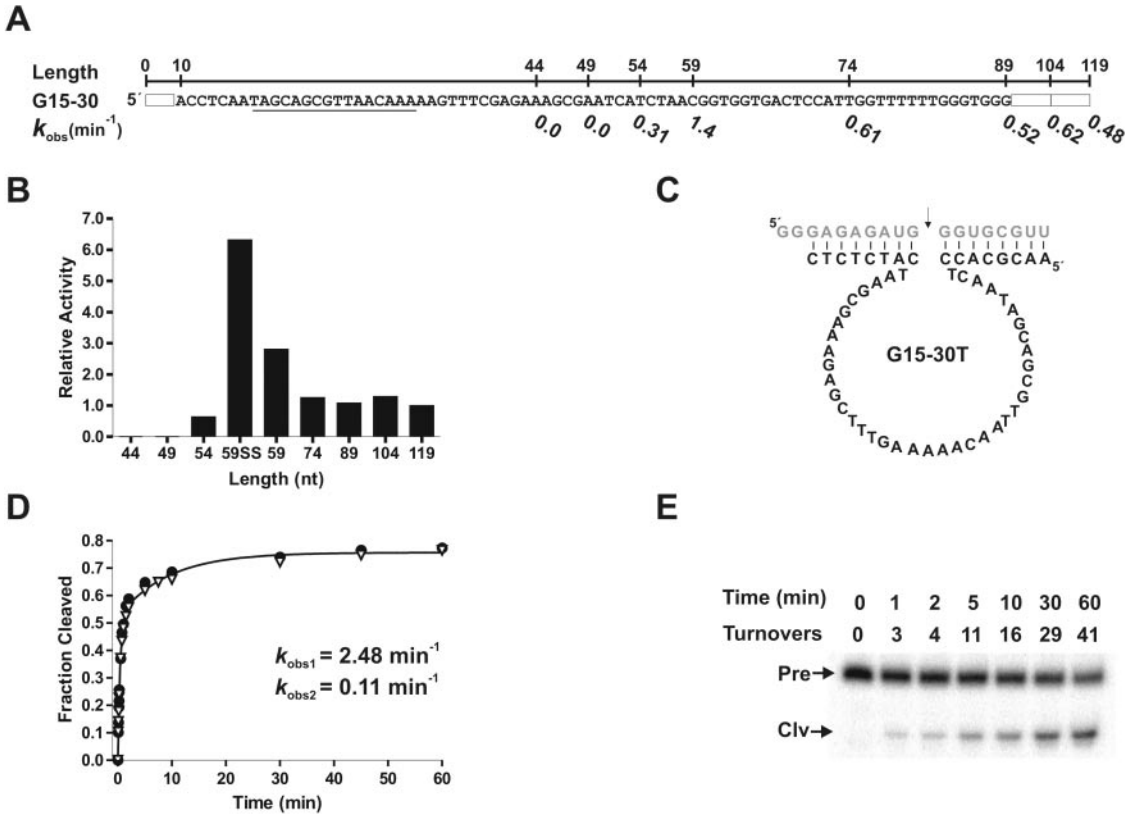

Figure 5. (**A**) Sequence of G15-30 and the corresponding k_{obs} values for various truncation derivatives. The numbers on top indicate the nucleotide length of various truncated versions, and the corresponding k_{obs} value is depicted below the sequence. Each k_{obs} value is the average of two independent trials, which typically differed by <20%. For simplicity, primer-binding sites are depicted as boxes. The underlined region shows some resemblance to an 8–17 motif, but does not satisfy all sequence requirements. (**B**) Relative activity of truncated deoxyribozymes. The activity of the 119 nt deoxyribozyme is taken as 1. Construct 59SS represents the 59 nt deoxyribozyme attached to the same truncated RNA substrate described previously. (**C**) Design of a shorter, trans-acting version of the G15-30 deoxyribozyme (G15-30T), and a shorter 18 nt RNA substrate (ST). (**D**) Kinetic analysis of G15-30T under single-turnover conditions (deoxyribozyme:substrate ratio of 100:1). The black line represents the non-linear least-squares fit to the experimental data using a double exponential equation ($R^2 = 0.997$). Two independent trials were conducted (trial 1, black circles; trial 2, white triangles), which differed by <10%. The rate constants k_{obs1} and k_{obs2} refer to the first and second phases, respectively. (**E**) Autoradiogram of trans cleavage assay for G15-30T conducted under multiple turnover conditions. A 100 fold excess of 5′-^{32}P-labelled substrate was incubated with G15-30T. Reaction conditions; 1 μM substrate, 10 nM enzyme and 50 mM HEPES (pH 7.0, at 23°C), 400 mM NaCl, 100 mM KCl, 7.5 mM $MnCl_2$, 7.5 mM $MgCl_2$, at room temperature; sampled at 0, 1, 2, 5, 10, 30 and 60 min. Cleavage products (Clv) were separated from the uncleaved precursor substrate (Pre) by electrophoresis in a denaturing 10% polyacrylamide gel.

alternative conformations. Interestingly, the 3′-truncated versions of each deoxyribozyme exhibit monophasic kinetics, which suggests that the extra nucleotides may facilitate the formation of alternative structures and the observed biphasic kinetics (Figure 4).

The 8–17 motifs of all sequence classes are listed in Supplementary Figure 2, and are grouped into four primary phenotypic classes (based on the relative activity scheme described in Figure 2A). Although we have listed 22 other 8–17 variants in the same general phenotypic class as G15-1, G15-16 and G15-39, it should be noted that these classes are still likely to be diverse in activity, and further subdivision has not been attempted due to insufficient mutational data. However, we do not expect that any of these classes died out due to an uncharacteristically large inhibitory effect from excess sequence elements. We identified two classes (G7-E129 and G10-E36.2) that closely resemble the fastest characterized 8–17 variant (i.e. identical to G15-16 but lacking one of the terminal adenosine residues and containing a different 3′ substrate-binding arm), yet died out in generation 7 and 10, respectively. The full-length version of G7-E129 was assayed for self-cleavage yielding a k_{obs} of 0.58 min^{-1} and Y_{max} of 61%, which provides further evidence that the results from our sample set are likely representative of the general population. At this time, we can only speculate as to why G7-E129 was eliminated so early in the selection, despite having catalytic properties comparable to G15-49 ($k_{obs} = 0.56$ min^{-1}, $Y_{max} = 65\%$). Other factors, such as PCR amplification bias, random genetic drift, and sampling error may have contributed to the loss of this sequence class. We have previously initiated an investigation into the population dynamics of *in vitro* selection, and expect future reports to yield even greater insight into the significance of these factors on the outcome of selection (41).

Characterization of a non-8–17 motif

From a total of 110 sequence classes isolated in our previous selection experiment, only seven did not appear to contain the 8–17 motif or any other previously reported RNA-cleaving

deoxyribozyme motif. Five of these classes were eliminated by generation 8, and another class was observed as a single clone in G13. Only one class (G15-30) survived the stringent 5 s selection pressure applied in G15, and represented ~10% of the population (from a sample of 49 clones). G15-30 was therefore selected for further examination. It should be noted that this class does possess some of the characteristic sequence requirements of 8–17 near the 5′ end, but lacks the strictly conserved G_{14} residue from the single-stranded turn region described in Figure 2A. Despite this discrepancy we originally suggested that catalysis in G15-30 [referred to previously as DZ4 in reference (33)], might still be supported by an unusual 8–17 variant. However, subsequent evidence from a more rigorous investigation supports the contrary. Multiple truncation tests were carried out to determine the minimal sequence requirements and the effect of excess sequence elements on G15-30. Figure 5A shows the nucleotide sequence of G15-30 and the catalytic rate constant associated with different truncated versions. The full-length molecule possesses a k_{obs} of 0.48 min^{-1}, but deleting 60 nt from the 3′ end leads to a k_{obs} of 1.4 min^{-1}. Further deletion causes a reduction in activity, with no activity being observed after an additional 10 nt are removed. The relative activity of the various deletion constructs are illustrated in Figure 5B. Point mutations were also introduced into the 59 nt version at positions expected to be crucial for activity, if 8–17 was indeed responsible for catalysis. However, a 5′ G22T mutant exhibited a k_{obs} of 1.1 min^{-1}, and a 5′ C29T mutant exhibited a k_{obs} of 0.28 min^{-1}, indicating that G15-30 does not utilize an 8–17 motif. Remarkably, the 59 nt version of G15-30 in conjunction with a truncated RNA substrate (59SS) is about 6-fold more active than the original 119 nt version. We used mfold to facilitate the design of a trans-acting version, called G15-30T, that engages a shortened RNA substrate through the formation of two duplex stems flanking the cleavage site (Figure 5C). The P1 primer-binding site is predicted to act as part of the 5′ substrate-binding arm of G15-30T, thereby defining the boundaries of the minimal catalytic core. Nevertheless, additional confirmatory deletion tests were conducted on the 5′ end of this trans-acting deoxyribozyme, and the results were consistent with the proposed structure model (data not shown). Under single-turnover conditions, G15-30T exhibits biphasic kinetics with a k_{obs} of 2.48 min^{-1} (Y_{max} = 52%) in the first phase, and 0.11 min^{-1} (Y_{max} = 24%) in the second phase (Figure 5D). G15-30T is also capable of multiple substrate turnovers. Over a 60 min incubation period, in the presence of 10 nM deoxyribozyme and 1 μM substrate, ~41% of substrate was cleaved corresponding to 41 turnovers (Figure 5E). Further characterization and optimization of G15-30T represents a future objective.

DISCUSSION

Herein, we have investigated the effects of excess sequence elements on a sample of RNA-cleaving deoxyribozymes isolated from a prior *in vitro* selection experiment. Despite an overall length of ~119 nt, we have provided evidence indicating that catalysis in 10 of these long deoxyribozymes is supported by the short 8–17 motif. Presumably, this finding is also true for ~94% of the 110 sequence classes previously isolated, which also contain variants of the 8–17 motif. Moreover, we have demonstrated that excess sequence elements in both the deoxyribozyme and substrate domains have only a minimal effect on activity (positive or negative), suggesting that these 8–17 motifs survived increasing selection pressure despite the presence of excess sequence elements, rather than because of them. In contrast, only a few new deoxyribozymes were identified, and only one of these (G15-30) could compete with 8–17 under stringent time pressure. A minimized version of this deoxyribozyme is ~2.5 times larger than 8–17, and experienced a ~4-fold greater inhibitory effect from excess sequence elements than the average 8–17 motif. Collectively, these results suggest that 8–17 may be less susceptible to the potential inhibitory effect of excess sequence elements than larger motifs, which could help to account for its widespread recurrence. However, a more systematic study is necessary to confirm this hypothesis. It remains possible that the minimal effects observed herein could be an artifact of the relative location of the 8–17 motifs, all of which were found at the 5′ end of the DNA domain. Additional factors including a large catalytic rate, a compact size, loose sequence requirements, substrate cleavage versatility and metal ion cofactor versatility, make 8–17 arguably one of the best solutions to deoxyribozyme mediated RNA-cleavage during *in vitro* selection. For these reasons, we suspect this motif will continue to 'hijack' future *in vitro* selection experiments, and hinder the discovery of novel RNA-cleaving deoxyribozymes. Not unlike 8–17, other simple functional motifs, such as the isoleucine RNA aptamer (42,43), ATP binding DNA aptamer (44), hammerhead ribozyme (45,46) and a small RNA ligase deoxyribozyme (13) have also been isolated on more than one occasion through *in vitro* selection. The general factors that influence the likelihood of recurrence have been addressed elsewhere (47).

The work presented herein complements the results of a previous study that also sought to characterize the effect of excess arbitrary sequence, using RNA ligase ribozymes as a model system (6). Our results provide additional support to indicate that the potential inhibitory effect of excess arbitrary sequence does not represent a significant deterrent against the use of longer random libraries. However, we were not able to reconcile the purported theoretical advantage of longer random libraries with our experimental outcome, in which a majority of small catalysts were isolated that did not significantly utilize additional nucleotides to their benefit. To date, 18 other *in vitro* selection experiments have been conducted for the purpose of isolating RNA-cleaving deoxyribozymes, and the average length of the random-sequence domain has been ~46 nt (10,11,27,28,30,32,38,48–58). By exploiting a library with ~30 additional random-sequence nucleotides, we originally expected a higher degree of structural diversity in the resulting population of catalysts. The recurrence of 8–17 in this study and elsewhere, alludes to the rarity of novel RNA-cleaving motifs (with comparable or higher activity) and/or reflects the limitations in our ability to access them through *in vitro* selection. A recent computational study that used graph theory to characterize the distribution of possible secondary structure motifs associated with various library lengths, has shown that typical library sizes strongly favour simple topological structures (59). Although structural complexity was shown to increase with library length, the actual benefit

was very small even for libraries as long as 100 nt. The prevalence of 8–17 in our study is consistent with these findings, and suggests that 80 random nucleotides may still represent a sub-optimal length for finding new, complex, and more efficient RNA-cleaving deoxyribozymes. Of course, the benefits of increasing the length of the random-sequence domain may be irrelevant, if the limiting factor is actually the relatively permissive reaction time ($\geq$5 s) that can be imposed as a selection constraint by conventional manual quenching techniques, and/or the small fraction of sequence space that can be searched in any single experiment. These constraints could potentially be overcome as automated SELEX (60–63) and continuous evolution (64) strategies become more widely applicable. In the meantime, case studies such as this one will continue to provide significant clues to the global distribution of deoxyribozymes in sequence space and underscore the current limitations in accessing them.

SUPPLEMENTARY DATA

Supplementary Data are available at NAR online.

ACKNOWLEDGEMENTS

This work was supported by a research grant from the Canadian Institutes for Health Research. Y.L. is a Canada research chair. K.S. is a former OGS recipient, and currently holds an NSERC CGS doctoral award. Funding to pay the Open Access publication charges for this article was provided by Canadian Institutes of Health Research.

Conflict of interest statement. None declared.

REFERENCES

1. Tuerk,C. and Gold,L. (1990) Systematic evolution of ligands by exponential enrichment: RNA ligands to bacteriophage T4 DNA polymerase. *Science*, **249**, 505–510.
2. Robertson,D.L. and Joyce,G.F. (1990) Selection *in vitro* of an RNA enzyme that specifically cleaves single-stranded DNA. *Nature*, **344**, 467–468.
3. Ellington,A.D. and Szostak,J.W. (1990) *In vitro* selection of RNA molecules that bind specific ligands. *Nature*, **346**, 818–822.
4. Knight,R., De Sterck,H., Markel,R., Smit,S., Oshmyansky,A. and Yarus,M. (2005) Abundance of correctly folded RNA motifs in sequence space, calculated on computational grids. *Nucleic Acids Res*., **33**, 5924–5935.
5. Knight,R. and Yarus,M. (2003) Finding specific RNA motifs: function in a zeptomole world? *RNA*, **9**, 218–230.
6. Sabeti,P.C., Unrau,P.J. and Bartel,D.P. (1997) Accessing rare activities from random RNA sequences: the importance of the length of molecules in the starting pool. *Chem. Biol*., **4**, 767–774.
7. Carothers,J.M., Oestreich,S.C., Davis,J.H. and Szostak,J.W. (2004) Informational complexity and functional activity of RNA structures. *J. Am. Chem. Soc*., **126**, 5130–5137.
8. Achenbach,J.C., Jeffries,G.A., McManus,S.A., Billen,L.P. and Li,Y. (2005) Secondary-structure characterization of two proficient kinase deoxyribozymes. *Biochemistry*, **44**, 3765–3774.
9. Kandadai,S.A. and Li,Y. (2005) Characterization of a catalytically efficient acidic RNA-cleaving deoxyribozyme. *Nucleic Acids Res*., **33**, 7164–7175.
10. Liu,Z., Mei,S.H., Brennan,J.D. and Li,Y. (2003) Assemblage of signaling DNA enzymes with intriguing metal-ion specificities and pH dependences. *J. Am. Chem. Soc*., **125**, 7539–7545.
11. Mei,S.H., Liu,Z., Brennan,J.D. and Li,Y. (2003) An efficient RNA-cleaving DNA enzyme that synchronizes catalysis with fluorescence signaling. *J. Am. Chem. Soc*., **125**, 412–420.
12. Shen,Y., Brennan,J.D. and Li,Y. (2005) Characterizing the secondary structure and identifying functionally essential nucleotides of pH6DZ1, a fluorescence-signaling and RNA-cleaving deoxyribozyme. *Biochemistry*, **44**, 12066–12076.
13. Prior,T.K., Semlow,D.R., Flynn-Charlebois,A., Rashid,I. and Silverman,S.K. (2004) Structure-function correlations derived from faster variants of a RNA ligase deoxyribozyme. *Nucleic Acids Res*., **32**, 1075–1082.
14. Fusz,S., Eisenfuhr,A., Srivatsan,S.G., Heckel,A. and Famulok,M. (2005) A ribozyme for the aldol reaction. *Chem. Biol*., **12**, 941–950.
15. Baskerville,S. and Bartel,D.P. (2002) A ribozyme that ligates RNA to protein. *Proc. Natl Acad. Sci. USA*, **99**, 9154–9159.
16. Zinnen,S.P., Domenico,K., Wilson,M., Dickinson,B.A., Beaudry,A., Mokler,V., Daniher,A.T., Burgin,A. and Beigelman,L. (2002) Selection, design, and characterization of a new potentially therapeutic ribozyme. *RNA*, **8**, 214–228.
17. Seelig,B. and Jaschke,A. (1999) A small catalytic RNA motif with Diels-Alderase activity. *Chem. Biol*., **6**, 167–176.
18. Chapman,K.B. and Szostak,J.W. (1995) Isolation of a ribozyme with 5′-5′ ligase activity. *Chem. Biol*., **2**, 325–333.
19. Jayasena,V.K. and Gold,L. (1997) *In vitro* selection of self-cleaving RNAs with a low pH optimum. *Proc. Natl Acad. Sci. USA*, **94**, 10612–10617.
20. Jenne,A. and Famulok,M. (1998) A novel ribozyme with ester transferase activity. *Chem. Biol*., **5**, 23–34.
21. Landweber,L.F. and Pokrovskaya,I.D. (1999) Emergence of a dual-catalytic RNA with metal-specific cleavage and ligase activities: the spandrels of RNA evolution. *Proc. Natl Acad. Sci. USA*, **96**, 173–178.
22. Sengle,G., Eisenfuhr,A., Arora,P.S., Nowick,J.S. and Famulok,M. (2001) Novel RNA catalysts for the Michael reaction. *Chem. Biol*., **8**, 459–473.
23. Ekland,E.H. and Bartel,D.P. (1995) The secondary structure and sequence optimization of an RNA ligase ribozyme. *Nucleic Acids Res*., **23**, 3231–3238.
24. Ekland,E.H., Szostak,J.W. and Bartel,D.P. (1995) Structurally complex and highly active RNA ligases derived from random RNA sequences. *Science*, **269**, 364–370.
25. Chapple,K.E., Bartel,D.P. and Unrau,P.J. (2003) Combinatorial minimization and secondary structure determination of a nucleotide synthase ribozyme. *RNA*, **9**, 1208–1220.
26. Tsukiji,S., Pattnaik,S.B. and Suga,H. (2003) An alcohol dehydrogenase ribozyme. *Nature Struct. Biol*., **10**, 713–717.
27. Li,J., Zheng,W., Kwon,A.H. and Lu,Y. (2000) *In vitro* selection and characterization of a highly efficient Zn(II)-dependent RNA-cleaving deoxyribozyme. *Nucleic Acids Res*., **28**, 481–488.
28. Faulhammer,D. and Famulok,M. (1996) The Ca2+ ion as a cofactor for a novel RNA-cleaving deoxyribozyme. *Angew Chem. Int. Ed Engl*., **35**, 2809–2813.
29. Faulhammer,D. and Famulok,M. (1997) Characterization and divalent metal-ion dependence of *in vitro* selected deoxyribozymes which cleave DNA/RNA chimeric oligonucleotides. *J. Mol. Biol*., **269**, 188–202.
30. Cruz,R.P., Withers,J.B. and Li,Y. (2004) Dinucleotide junction cleavage versatility of 8-17 deoxyribozyme. *Chem. Biol*., **11**, 57–67.
31. Peracchi,A. (2000) Preferential activation of the 8-17 deoxyribozyme by Ca(2+) ions. Evidence for the identity of 8-17 with the catalytic domain of the Mg5 deoxyribozyme. *J. Biol. Chem*., **275**, 11693–11697.
32. Santoro,S.W. and Joyce,G.F. (1997) A general purpose RNA-cleaving DNA enzyme. *Proc. Natl Acad. Sci. USA*, **94**, 4262–4266.
33. Schlosser,K. and Li,Y. (2004) Tracing sequence diversity change of RNA-cleaving deoxyribozymes under increasing selection pressure during *in vitro* selection. *Biochemistry*, **43**, 9695–9707.
34. Peracchi,A., Bonaccio,M. and Clerici,M. (2005) A mutational analysis of the 8-17 deoxyribozyme core. *J. Mol. Biol*., **352**, 783–794.
35. Bonaccio,M., Credali,A. and Peracchi,A. (2004) Kinetic and thermodynamic characterization of the RNA-cleaving 8-17 deoxyribozyme. *Nucleic Acids Res*., **32**, 916–925.
36. Hertel,K.J., Pardi,A., Uhlenbeck,O.C., Koizumi,M., Ohtsuka,E., Uesugi,S., Cedergren,R., Eckstein,F., Gerlach,W.L., Hodgson,R. *et al*. (1992) Numbering system for the hammerhead. *Nucleic Acids Res*., **20**, 3252.

37. Zuker,M. (2003) Mfold web server for nucleic acid folding and hybridization prediction. *Nucleic Acids Res*., **31**, 3406–3415.
38. Ordoukhanian,P. and Joyce,G.F. (2002) RNA-cleaving DNA enzymes with altered regio- or enantioselectivity. *J. Am. Chem. Soc*., **124**, 12499–12506.
39. Esteban,J.A., Banerjee,A.R. and Burke,J.M. (1997) Kinetic mechanism of the hairpin ribozyme. Identification and characterization of two nonexchangeable conformations. *J. Biol. Chem*., **272**, 13629–13639.
40. Esteban,J.A., Walter,N.G., Kotzorek,G., Heckman,J.E. and Burke,J.M. (1998) Structural basis for heterogeneous kinetics: reengineering the hairpin ribozyme. *Proc. Natl Acad. Sci. USA*, **95**, 6091–6096.
41. Schlosser,K. and Li,Y. (2005) Diverse evolutionary trajectories characterize a community of RNA-cleaving deoxyribozymes: a case study into the population dynamics of *in vitro* selection. *J. Mol. Evol*., **61**, 192–206.
42. Legiewicz,M., Lozupone,C., Knight,R. and Yarus,M. (2005) Size, constant sequences, and optimal selection. *RNA*, **11**, 1701–1709.
43. Lozupone,C., Changayil,S., Majerfeld,I. and Yarus,M. (2003) Selection of the simplest RNA that binds isoleucine. *RNA*, **9**, 1315–1322.
44. Nutiu,R. and Li,Y. (2005) *In vitro* selection of structure-switching signaling aptamers. *Angew Chem. Int. Ed. Engl*., **44**, 1061–1065.
45. Salehi-Ashtiani,K. and Szostak,J.W. (2001) *In vitro* evolution suggests multiple origins for the hammerhead ribozyme. *Nature*, **414**, 82–84.
46. Tang,J. and Breaker,R.R. (2000) Structural diversity of self-cleaving ribozymes. *Proc. Natl Acad. Sci. USA*, **97**, 5784–5789.
47. Lehman,N. (2004) Assessing the likelihood of recurrence during RNA evolution *in vitro*. *Artif Life*, **10**, 1–22.
48. Breaker,R.R. and Joyce,G.F. (1994) A DNA enzyme that cleaves RNA. *Chem. Biol*., **1**, 223–229.
49. Breaker,R.R. and Joyce,G.F. (1995) A DNA enzyme with Mg(2+)-dependent RNA phosphoesterase activity. *Chem. Biol*., **2**, 655–660.
50. Carrigan,M.A., Ricardo,A., Ang,D.N. and Benner,S.A. (2004) Quantitative analysis of a RNA-cleaving DNA catalyst obtained via *in vitro* selection. *Biochemistry*, **43**, 11446–11459.
51. Feldman,A.R. and Sen,D. (2001) A new and efficient DNA enzyme for the sequence-specific cleavage of RNA. *J. Mol. Biol*., **313**, 283–294.
52. Geyer,C.R. and Sen,D. (1997) Evidence for the metal-cofactor independence of an RNA phosphodiester-cleaving DNA enzyme. *Chem. Biol*., **4**, 579–593.
53. Santoro,S.W., Joyce,G.F., Sakthivel,K., Gramatikova,S. and Barbas,C.F.,IIIrd. (2000) RNA cleavage by a DNA enzyme with extended chemical functionality. *J. Am. Chem. Soc*., **122**, 2433–2439.
54. Roth,A. and Breaker,R.R. (1998) An amino acid as a cofactor for a catalytic polynucleotide. *Proc. Natl Acad. Sci. USA*, **95**, 6027–6031.
55. Nelson,K.E., Bruesehoff,P.J. and Lu,Y. (2005) *In vitro* selection of high temperature Zn(2+)-dependent DNAzymes. *J. Mol. Evol*., **61**, 216–225.
56. Sidorov,A.V., Grasby,J.A. and Williams,D.M. (2004) Sequence-specific cleavage of RNA in the absence of divalent metal ions by a DNAzyme incorporating imidazolyl and amino functionalities. *Nucleic Acids Res*., **32**, 1591–1601.
57. Perrin,D.M., Garestier,T. and Helene,C. (2001) Bridging the gap between proteins and nucleic acids: a metal-independent RNAseA mimic with two protein-like functionalities. *J. Am. Chem. Soc*., **123**, 1556–1563.
58. Bruesehoff,P.J., Li,J., Augustine,A.J. 3rd and Lu,Y. (2002) Improving metal ion specificity during in vitro selection of catalytic DNA. *Comb Chem High Throughput Screen*, **5**, 327–335.
59. Gevertz,J., Gan,H.H. and Schlick,T. (2005) *In vitro* RNA random pools are not structurally diverse: a computational analysis. *RNA*, **11**, 853–863.
60. Cox,J.C., Rudolph,P. and Ellington,A.D. (1998) Automated RNA selection. *Biotechnol. Prog*., **14**, 845–850.
61. Cox,J.C., Rajendran,M., Riedel,T., Davidson,E.A., Sooter,L.J., Bayer,T.S., Schmitz-Brown,M. and Ellington,A.D. (2002) Automated acquisition of aptamer sequences. *Comb Chem. High Throughput Screen*, **5**, 289–299.
62. Drolet,D.W., Jenison,R.D., Smith,D.E., Pratt,D. and Hicke,B.J. (1999) A high throughput platform for systematic evolution of ligands by exponential enrichment (SELEX). *Comb Chem. High Throughput Screen*, **2**, 271–278.
63. Eulberg,D., Buchner,K., Maasch,C. and Klussmann,S. (2005) Development of an automated *in vitro* selection protocol to obtain RNA-based aptamers: identification of a biostable substance P antagonist. *Nucleic Acids Res*., **33**, e45.
64. Johns,G.C. and Joyce,G.F. (2005) The promise and peril of continuous *in vitro* evolution. *J. Mol. Evol*., **61**, 253–263.